A generalized advancing front model describing the oxygen transfer in flowing blood

A GENERALIZED ADVANCING FRONT MODEL DESCRIBING THE OXYGEN TRANSFER IN FLOWING BLOOD

J.M.M. Oomens and J.A.E. Spaan

Department of Mechanical Engeneering, University of Technology, Eindhoven, the Netherlands

INTRODUCTION

It is well known from literature that under certain conditions the steady state transport of oxygen in flowing blood can be described relatively simple when a sharp boundary (advancing front) is assumed between oxygenated and unoxygenated blood (4). Advancing Front (A F) theories have been used to predict oxygen transfer rates in membrane oxygenators (e.g. 2,5). Advancing Front models presented in literature (2,3,4,5,6) have been derived for specific geometries of the flow channel and well defined velocity profiles. A general A F theory would be useful to predict oxygen transport performance for the variety of flow geometries and flow conditions encountered in experimental studies with membrane oxygenators and to analyse the data of existing oxygenators. In this work a general A F theory is presented.

The derivation of the more general A F theory will be done for an oxygenation situation as given in Fig. 1 and under the following conditions: the flow in the oxygenation channel is fully developed laminair flow, the hemoglobin distribution in the blood is considered to be uniform, the diffusion of oxygen in the flow direction is neglected with respect to the diffusion perpendicular to the flow, the oxygen tension outside the flow channel is constant, and the diffusion of hemoglobin and oxyhemoglobin is neglected. The basic assumptions for the A F theory are the following: the oxygenation reaction is instantaneous, a large difference exists between the initial oxygen partial pressure in the blood and the partial pressure in the gas side, and the oxygen flux through the membrane and the saturated blood layer is considered to be constant by given z*.

MASS TRANSFER EQUATIONS

The dimensionless transfer equations which determine the O_2 transfer in flowing blood can be given by (1,2,3 and 6)

$$\frac{\partial^2 C}{\partial x^{*2}} = f(x^*)\cdot\frac{\partial}{\partial z^*}(C + h.S) \qquad \text{flat duct} \quad (1)$$

$$\frac{1}{r^*}\cdot\frac{\partial}{\partial r^*}\left(r^*\cdot\frac{\partial C}{\partial r^*}\right) = f(r^*)\cdot\frac{\partial}{\partial z^*}(C+h.S) \qquad \text{tube} \quad (2)$$

Equations 1 and 2 represent a differential mass balance where at steady state the diffusion of oxygen into a blood volume is balanced against the convective removal. In the above equations z^*; $f(x^*)$, $f(r^*)$; and x^*, r^* are the dimensionless flow channel length, the dimensionless velocity profile, and the depth in the blood layer, respectively, and are given by

flat duct		tube	
$z^* = \frac{z.Dv}{d^2.\bar{V}}$	(3)	$z^* = \frac{z.Dv}{R^2.\bar{V}}$	(4)
$f(x^*) = V_z(x)/\bar{V}$	(5)	$f(r^*) = V_z(r)/\bar{V}$	(6)
$x^* = x/d$	(7)	$r^* = r/R$	(8)

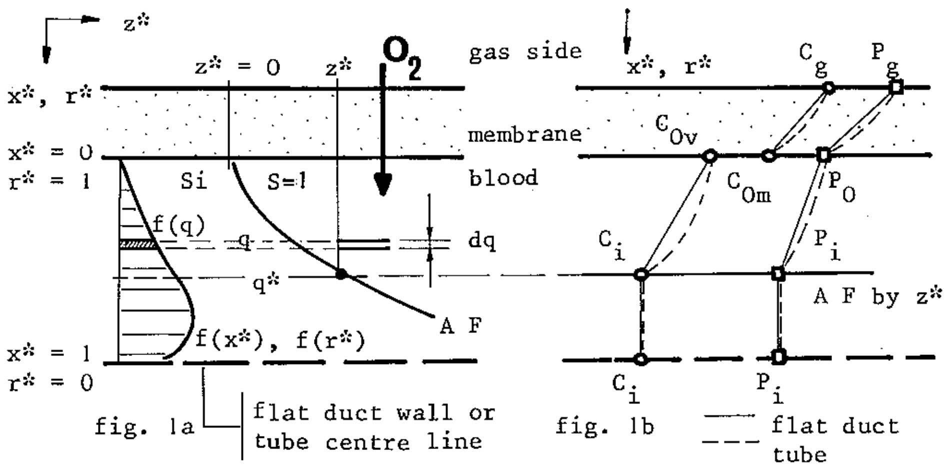

Figure 1. Schematic diagram of an oxygenation channel. The blood is separated from the gas side by a permeable membrane.

a) Path of the A F front with a general velocity profile.

b) Corresponding O_2 concentration-partial pressure profiles in the blood and the membrane by given channel length z^*.

The corresponding boundary conditions for equations 1 and 2 are (see also figure 1)

flat duct		tube	
All x^*; $z^*<0$; $C = C_i$	(9)	All r^*; $z^*<0$; $C = C_i$	(10)
blood membrane interface			
$C_{ov}/\alpha_v = C_{om}/\alpha_m$	(11)	$C_{ov}/\alpha_v = C_{om}/\alpha_m$	(12)
$x^*=0; z^*\geq 0; D_v(\frac{\partial C}{\partial x^*}) = D_m(\frac{\partial C}{\partial x^*})$	(13)	$r^*=1; z^*\geq 0; D_v(\frac{\partial C}{\partial r^*}) = D_m(\frac{\partial C}{\partial r^*})$	(14)
conditions of no flux in the solid wall or center line			
$x^*=1$; All z^*; $D_v\frac{\partial C}{\partial x^*}=0$	(15)	$r^*=0$; All z^*; $D_v\frac{\partial C}{\partial r^*}=0$	(16)

Because of the A F assumptions the following equations obtain within the saturated part of the blood layer

$$\frac{d}{dx^*}\left[D_{v,m}\left(\frac{dC}{dx^*}\right)\right] = 0 \quad (17) \qquad \frac{d}{dr^*}\left[r^*\cdot D_{v,m}\left(\frac{dC}{dr^*}\right)\right] = 0 \quad (18)$$

Integration of equations 17 and 18 result in the following formulas for the O_2 concentration profiles

$$C = C_i+(C_{ov}-C_i)(1-\frac{x^*}{q^*}) \quad (19) \qquad C = C_i\cdot\frac{\ln r^*}{\ln q^*} + C_{ov}(1-\frac{\ln r^*}{\ln q^*}) \quad (20)$$

The A F equations may be obtained by integration of the differential equations 1 and 2, from the blood membrane interface to the A F and from the front to the unpermeable wall respectively the tube centre line (6). In performing the integration procedure, the O_2 concentration and saturation profiles as well as the boundary conditions have to be used. This results for the tube in

$$dz^*=\left[H\cdot q\cdot f(q)(\ln q-2M)+\frac{1}{q(\ln q-2M)}\left(\int_0^{q^*} q\cdot\ln q\cdot f(q)dq-2M\cdot\int_0^{q^*} q\cdot f(q)dq\right)\right]dq \quad (21)$$

The flow averaged saturation at a dimensionless distance z^* is

$$\overline{S} = 2\cdot\int_{q^*}^{1} q\cdot f(q)dq + S_i\cdot 2\int_0^{q^*} q\cdot f(q)\cdot dq \quad (22)$$

Integration of equation 21 together with 22 results in the general A F model for the tube. It is given in terms of four dimensionless numbers L^*, H, M, and f and three integral formulas I_1, I_2 and I_3. For the flat duct and the tube the general A F equations become

$$\boxed{L^*=H(I_2+M\ I_1)+I_3} \quad (23) \qquad \boxed{f = I_1} \quad (24)$$

Where L^* is the dimensionless length of the flow channel, H is the ratio of the remaining O_2 uptake capacity of the entering blood and the concentration difference between the entering blood and the gas side, M is the relative membrane resistance, and f the fractional saturation change. I_1, I_2 and I_3 depend only on the velocity profile and the chosen flow channel geometry. Equations 23 and 24 are presented for a general velocity profile and geometry of the flow channel. Tabel I gives an overview and comparison of the terms of the equations for the tube and the flat duct geometry. Equation 23 can be subdivided in three characteristic parts wich represent the three influences that determine the depth of penetration of the oxygenation front in the bloodlayer at a given dimensionless length of the flow channel L^*.

$H \cdot I_2$	represents chemical reaction	(23a)
$H \cdot M \cdot I_1$	represents the membrane resistance	(23b)
I_3	represents physically dissolved oxygen	(23c)

The effect of the membrane resistance or the physically dissolved oxygen can be neglected simply by setting M or I_3 equal to zero. Under normal conditions the chemical reaction term determines for 85% the required flow channel length, the membrane resistance for 10% and the physically dissolved oxygen for 5%. Therefore a closer examination of the integral term I_2 in the equation 23 is necessary.

The physical significance of the integral term I_2 and the effect of the velocity profile will be investigated for the flat duct geometry. I_2 can be defined from figure 1a as the dimensionless saturated flow moment. It is the sum of the flow in parallel differential saturated layers (f(q) dq) times the diffusion pathways q travelled by the O_2 to reach these layers,

$$I_2 = \Sigma\ (f(q)dq) \cdot q = \int_0^{q^*} q \cdot f(q)dq \qquad (41)$$

The saturated flow moment allows to quantify the (intuitive) supposition that a large part of the flow close along the blood gas interface achieves more effective oxygenation than flow far from this interface. In terms of a flow moment, one can say that by a fixed saturated flow (a fixed amount of O_2 uptake in the blood), the smaller I_2 the shorter the needed dimensionless flow channel length. Since I_2 is only determined (for a given f) by the function f(q) it is clear that the influence of f(q) on I_2 can be studied by a velocity distribution that depends on one parameter only in which the flow can be brought either close or far from the blood gas interface by change of that parameter. Such a velocity profile for example is represented by the formula

TUBE

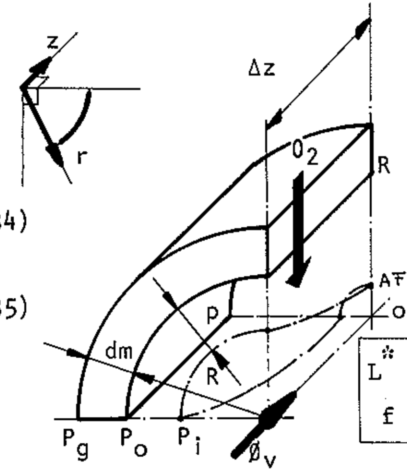

$$f(q) = \frac{V_{z(r)}}{\bar{V}} \quad (34)$$

$$q^* = \left(\frac{R-P}{R}\right) \quad (35)$$

$$f = \frac{\bar{S}-Si}{1-Si} \quad (27)$$

$$L^* = \frac{L \cdot D_v}{d^2 \cdot \bar{V}} \quad (28)$$

$$H = \frac{h \cdot (1-Si)}{(P_g - P_i)\alpha_v} \quad (29)$$

$$M = \frac{1}{2} \frac{\alpha_v . D_v}{\alpha_m . D_m} \ln\left(1 + \frac{dm}{R}\right) \quad (30)$$

$$I_1 = -2 \int_1^{q^*} q . f(q) dq \quad (31)$$

$$I_2 = \int_1^{q^*} q . \ln q . f(q) dq \quad (32)$$

$$I_3 = \int_0^{q^*} \frac{I_2 + MI_1}{q(\ln q - 2M)} dq \quad (33)$$

$$L^* = H(I_2 + MI_1) + I_3$$

$$f = I_1$$

FLAT DUCT

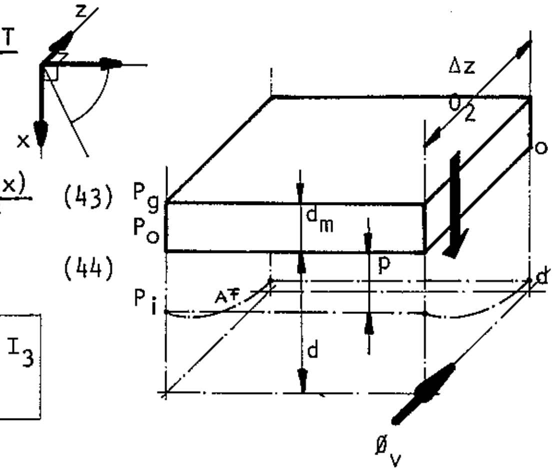

$$f(q) = \frac{V_{z(x)}}{\bar{V}} \quad (43)$$

$$q^* = \frac{p}{d} \quad (44)$$

$$f = \frac{\bar{S}-Si}{1-Si} \quad (36)$$

$$L^* = \frac{L . D_v}{R^2 . \bar{V}} \quad (37)$$

$$H = \frac{h \cdot (1-Si)}{(P_g - P_i)\alpha_v} \quad (38)$$

$$M = \frac{\alpha_v . D_v}{\alpha_m . D_m} \cdot \frac{dm}{d} \quad (39)$$

$$I_1 = \int_o^{q^*} f(q)\, dq \quad (40)$$

$$I_2 = \int_o^{q^*} q . f(q) dq \quad (41)$$

$$I_3 = \int_0^{q^*} \frac{I_2 + MI_1}{q + M} dq \quad (42)$$

TABLE I. Overview and Comparison of the Dimensionless Numbers and Integral Terms in the General A F Equations 23 and 24.

$$V_z(x)=A\cdot(\frac{x}{d})^n \qquad (45)$$

and the reversed function

$$V_z(x)=A\cdot(1-\frac{x}{d})^n \qquad (46)$$

with 0 = n = ∞ and coupled by n=0. The mean velocity for both profiles is given by

$$\bar{V} = A\cdot(\frac{1}{n+1}) \qquad (47)$$

$V_z(x)$ divided by $\bar{V}$ yields the dimensionless velocity function $f(x^*)$. For equation 45 and 46 $f(x^*)$ becomes respectively

$$f(x^*) = (n + 1)\cdot(x^*)^n \qquad (48)$$

$$f(x^*) = (n + 1)\cdot(1 - x^*)^n \qquad (49)$$

The corresponding integrals I_2 can be calculated for eq. 45 as

$$I_2=(n+1)\cdot\int_0^{q^*} q\cdot(q)^n\,dq = \left[(n+1)/(n+2)\right] q^{*\,n+2} \qquad (49)$$

and for 46 as

$$I_2=(n+1)\int_1^{q^*} q(1-q)^n dq=(n+1)/(n+2)\left[(1-q^*)^{n+2}-1\right]-\left[(1-q^*)^{n+1}-1\right] \qquad (50)$$

In figure 2, I_2 is given for several values f (equals I_1) as a function of the velocity parameter n. The upper part of figure 2 represents the velocity profiles for different values of n.

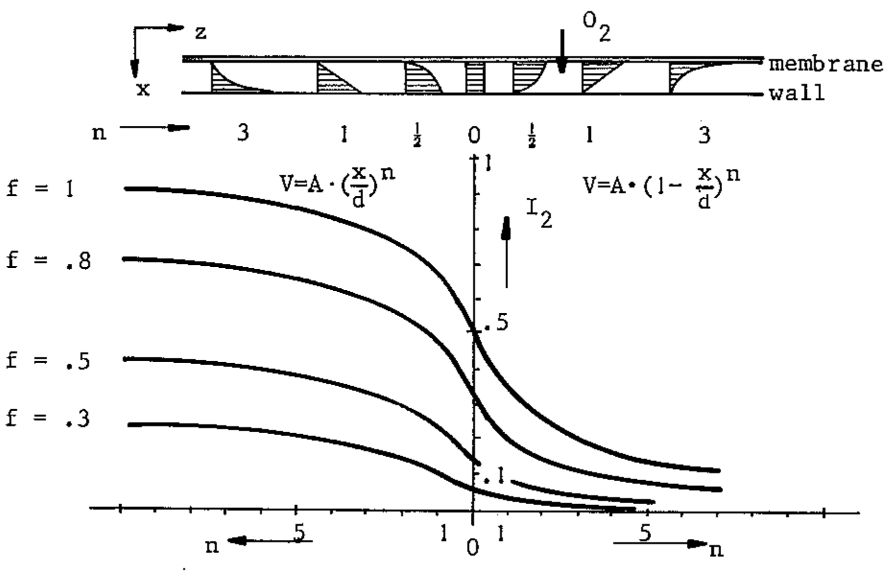

Figure 2 The variation of the flow moment with the velocity parameter for various values of the fractional saturation change.

It can easily be seen that the greater the flow along the membrane the better the oxygenation. There is a great change in the saturated flow moment for values of $n \leqslant 2$. This is also the region where such velocity profiles are encountered in existing membrane oxygenators. Plugflow is represented by $n=0$, nearly parabolic flow by $n=\frac{1}{2}$, shearflow by $n=1$, and nearly couette flow by $n=2$. In the development of an oxygenator the therm I_2 can be helpful in choosing an appropriate velocity profile for the device.

The general A F model presented here depends on situations where only one side of the flow channel is permeable to oxygen. For the case of membranes on both sides of the channel, eq. 23 and 24 and the equations in tabel I are still applicable. With symmetrical flow in such a channel, the penetration depth q now varies between 0 and $\frac{1}{2}$. The problem of membranes on both sides and an asymmetric flow profile in the channel can be solved by utilizing the one membrane equations presented here and through the use of the appropriate velocity profiles one has to preform two calculations to determine the penetration depths q_1^* and q_2^* at either side of the membranes. The modelling of the two membrane channels by two one membrane channel is valid as long as $q_1^*+q_2^* \leqslant 1$. The blood is fully saturated when $q_1^*+q_2^*=1$. Similarly to figure 2 (when $I_3 . M=0$) I_2 as a function of n is given in figure 3 for $q_1^*+q_2^*=1$ (f=1). Comparison of figures 2 and 3 shows that a channel with membranes on both sides reduces the flow moment three to four times compared to the one membrane channel for the case $I_1=f=1$. For the region $n \leqslant 2$ the influence of the velocity profile on I_2 is not very significant. This is contrary to the behaviour shown in figure 2.

CONCLUSIONS

Derivation of A F equations from the generalised A F model (equations 23 and 24) for a given flow-oxygenation situation, reduces the question to the resolution of three simple integral formulas. The defined flow moment can be used to quantify the mean influence of the velocity profile on the dimensionless length of a flow channel.

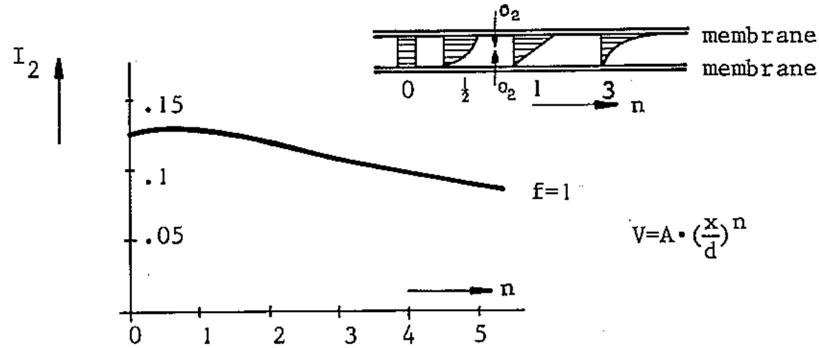

Figure 3. The influence of the flow parameter on the flow moment for the two membrane channels with an asymmetric velocity profile.

NOTATION

A = constant

α_m = solubility coeff. of O_2 in the membrane material

α_v = solubility coeff. of O_2 in blood plasma

C_g = O_2 concentration

C_i = initial oxygen concentration

C_{om} = O_2 concentration in the membrane at the blood interface

C_{ov} = O_2 concentration in the blood at the membrane interface

C = O_2 concentration

d = channel height

d_m = membrane thickness

D_m = diffusion coeff. of oxygen in membrane

D_v = diffusion coeff. of oxygen in blood

h = max O_2 binding capacity

L = lenght of the flow channel

n = velocity parameter

$\emptyset_v$ = blood flow rate

p = distance from the origin to the A F

P_g = constant partial pressure in the gas side

P_i = initial uniform partial pressure in the blood

P_o = partial pressure at the blood membrane interface

q^* = dimensionless distance from the origin to the A F

r = radius

R = inner radius of the tube

S = oxygen saturation

$\bar{S}$ = average oxygen saturation

S_i = initial oxygen saturation

$\bar{V}$ = mean velocity

V_z = local velocity

x = depth in the channel

z = distance along the flow channel

REFERENCES

1. Buckles, R.G., Merrill, E.W., and E.R. Gilliland, AIChE J., 14:703 (1968)
2. Dorson, W.J. Jr., Larsen, K.G., Elgas, R.J., and M.E. Voorhees, Trans. A.S.A.I.O., 17:309 (1971)
3. Dorson, W.J. Jr., in: Blood Oxygenation, D. Hershey, ed., Plenum Press, NY(1970) p 355-372
4. Lightfoot, E.N., AIChE J., 14,669 (1968)
5. Overcash, M.R., Ph. D. Thesis, University of Minnesota (1972)
6. Spaan, J.A.E., Pflügers Arch., 342, 289 (1973)

ACKNOWLEDGEMENTS

This work was partially supported by a grant from Stiftung Volkswagenwerk. Discussion with Dr. Pieter Stroeve about this paper is appreciated.